Decreased aminoacylation in pathology-related mutants of mitochondrial tRNA^{Tyr} is associated with structural perturbations in tRNA architecture

LUC BONNEFOND, CATHERINE FLORENTZ, RICHARD GIEGÉ, and JOËLLE RUDINGER-THIRION
Architecture et Réactivité de l'ARN, Université Louis Pasteur de Strasbourg, CNRS, 67084 Strasbourg, France

ABSTRACT

A growing number of human pathologies are ascribed to mutations in mitochondrial tRNA genes. Here, we report biochemical investigations on three mt-tRNA^{Tyr} molecules with point substitutions associated with diseases. The mutations occur in the atypical T- and D-loops at positions homologous to those involved in the tertiary interaction network of canonical tRNAs. They do not correspond to tyrosine identity positions and likely do not contact the mitochondrial tyrosyl-tRNA synthetase during the aminoacylation process. The impact of these substitutions on mt-tRNA^{Tyr} tyrosylation and structure was investigated using the corresponding tRNA transcripts. In vitro tyrosylation efficiency is decreased 600-fold for mutant A22G (mitochondrial gene mutation T5874C), 40-fold for G15A (C5877T), and is without significant effect on U54C (A5843G). Comparative solution probings with lead and nucleases on mutant and wild-type tRNA^{Tyr} molecules reveal a greater sensitivity to single-strand specific probes for mutants G15A and A22G. For both transcripts, the mutation triggers a structural destabilization in the D-loop that propagates toward the anticodon arm and thus hinders efficient tyrosylation. Further probing analysis combined with phylogenetic data support the participation of G15 and A22 in the tertiary network of human mt-tRNA^{Tyr} via nonclassical Watson–Crick G15–C48 and G13–A22 pairings. In contrast, the pathogenic effect of the tyrosylable mutant U54C, where structure is only marginally affected, has to be sought at another level of the tRNA^{Tyr} life cycle.

Keywords: aminoacylation; disease; mitochondria; tRNA^{Tyr}; tyrosyl-tRNA synthetase; structure probing

INTRODUCTION

A large number of mutations in human mitochondrial transfer RNA (mt-tRNA) genes have been correlated with degenerative disorders concerning brain, heart, muscles, eyes, kidneys, and endocrine glands (for review, see Wallace 1999; Chinnery and Turnbull 2000; Jacobs and Holt 2000). Since tRNAs are key molecules interacting with a variety of partners during the translational process, it is understandable that mutations can disturb various mitochondrial functions. Following this rationale, biochemical studies indeed revealed that pathogenic mutations can affect tRNAs at various steps including its structure, 3′-end maturation, post-transcriptional modifications, aminoacylation, complex formation with translation factors, association with ribosomes and decoding process (for review, see Florentz et al. 2003; Wittenhagen and Kelley 2003; Levinger et al. 2004; Taylor and Turnbull 2005). Presently, more than 130 mutations were described, distributed among all the 22 human mt-tRNA species encoded by the mitochondrial genome (see http://www.mitomap.org) (Brandon et al. 2005).

This report relates to the human mt-tRNA^{Tyr} gene in which three single substitutions lead to a set of diseases. The pathogenic mutations correspond to the single substitutions C5877T, T5874C, and A5843G in the mitochondrial genome that lead to familial chronic progressive external ophtalmoplegia (Sahashi et al. 2001), exercise intolerance associated with complex III deficiency (Pulkes et al. 2000), and mitochondrial cytopathy (Scaglia et al. 2003), respectively. The choice of studying human mt-tRNA^{Tyr} was dictated by several considerations. First, the recently solved crystal structure of the mt-TyrRS (Bonnefond et al. 2007a,b) makes it possible to present a model for the interaction of human mitochondrial tRNA^{Tyr} with mt-TyrRS, which help to understand the effects triggered by the mutations. Second, substitutions G15A, A22G, and

Reprint requests to: Joëlle Rudinger-Thirion, Architecture et Réactivité de l'ARN, Université Louis Pasteur de Strasbourg, CNRS, IBMC, 15 rue René Descartes, 67084 Strasbourg, France; e-mail: j.rudinger@ibmc.u-strasbg.fr; fax: 33 (0) 3 88 60 22 18.

Article published online ahead of print. Article and publication date are at http://www.rnajournal.org/cgi/doi/10.1261/rna.938108.

U54C in human mt-tRNA^{Tyr} occur in loops (Fig. 1A) in contrast to the majority (66%) of point mutations that are found in stem regions of mt-tRNAs (Florentz and Sissler 2001; McFarland et al. 2004). Third, up to date, basic research was essentially concentrated on four human mt-tRNAs genes that are "hotspots" for mutations (coding for tRNA$^{Leu(UUR)}$, tRNA^{Lys}, tRNA^{Ile}, and tRNA$^{Ser(UCN)}$) with no biochemical investigations on tRNA^{Tyr}. Finally, most studied mt-tRNAs belong to the "light"[1] tRNA family containing few G residues (e.g., human mt-tRNA$^{Leu(UUR)}$, tRNA^{Lys}, tRNA^{Ile}) and therefore are intrinsically fragile (Florentz et al. 2003), whereas tRNA^{Tyr} is a "heavy" tRNA anticipated to be more structured.

In this study, we investigate the impact of the three mt-tRNA^{Tyr} pathogenic substitutions using in vitro tyrosylation assays combined with solution probing experiments. We show that both D-loop mutations perturb the tRNA^{Tyr} tertiary folding and thereafter hinder efficient recognition by the homologous TyrRS. On the contrary, the T-loop mutation alters neither the global tRNA structure nor its tyrosylation properties. Altogether, the results presented allow us to propose a structural relationship between the D-loop and variable region in mt-tRNA^{Tyr} as well as two tertiary interactions.

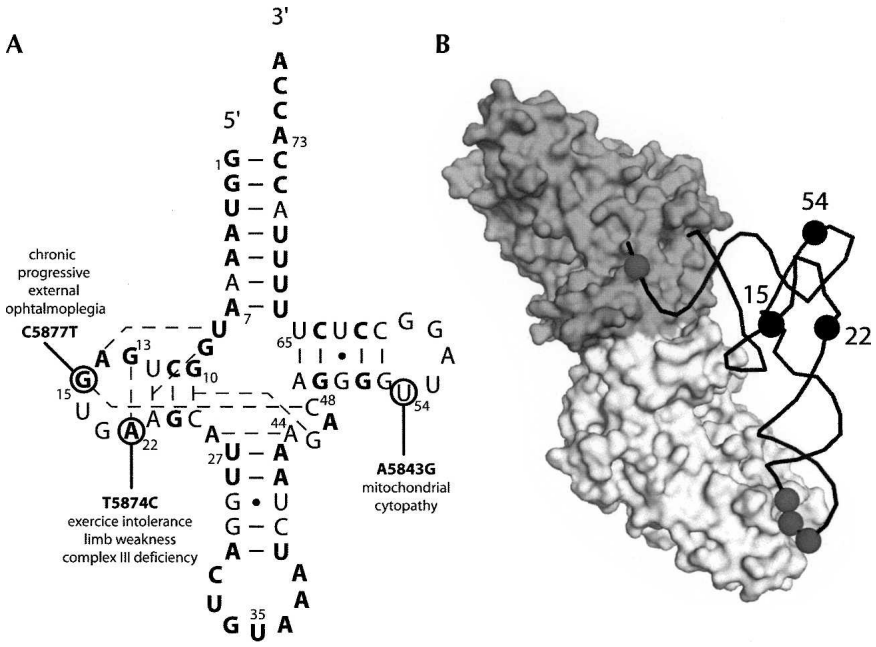

FIGURE 1. Location of pathology-related mutations in human mitochondrial tRNA^{Tyr}. (*A*) Model of secondary structure of human mt-tRNA^{Tyr}, a tRNA belonging to the "heavy" mt-tRNA family with 26% of G residues (Helm et al. 2000). Positions of pathogenic point substitutions, as found in mitochondrial DNA, are circled and the corresponding mutations in the gene with associated clinical effects are explicitly given. Dashed lines indicate putative tertiary interactions as proposed by Helm et al. (2000). Sequence data and numbering are according to Anderson et al. (1981) and Sprinzl and Vassilenko (2005), respectively. Residues in bold are those highly conserved (> 90%) in 150 mammalian mt-tRNA^{Tyr} species (Pütz et al. 2007). Notice that gene mutation A5843G, previously annotated C55 in mt-tRNA^{Tyr}, is considered in this work as C54 according to the mt-tRNA database numbering from Pütz et al. (2007). A fourth pathogenic mutant was not considered in this work since it concerns a nucleotide deletion in the acceptor stem (Raffelsberger et al. 2001). (*B*) Interaction model of human mt-TyrRS with tRNA. The mt-TyrRS crystal structure is from Bonnefond et al. (2007b); the homodimeric organization is emphasized by darkening one monomer. Docking of tRNA across both TyrRS subunits was achieved taking into account sequence and crystallographic knowledge of tyrosine systems (Bedouelle 2005). Gray dots show the tyrosine identity elements as determined by Bonnefond et al. (2005b), whereas black dots indicate location of the three pathogenic mutations on a tRNA backbone.

RESULTS AND DISCUSSION

Human mt-tRNA^{Tyr}

Comparison of the 150 mammalian mt-tRNA^{Tyr} sequences available (http://mamit-tRNA.u-strasbg.fr; Pütz et al. 2007) reveals 80% of conserved residues, especially located in stems and anticodon loop (Fig. 1A). Differences occur mainly in T- and D-loops that vary in sequence and size (D-loops from three to six nucleotides [nt]; T-loops from three to eight nt). Further, mammalian mt-tRNA^{Tyr} species do not contain a subset of nucleotides known to be involved in the tertiary interaction network of canonical tRNAs (Giegé et al. 1993). Thus, in the particular case of human mt-tRNA^{Tyr}, representative of mammalian tyrosine specific tRNAs (Fig. 1A), D-loop lacks the conserved G18–G19 dinucleotide usually involved in two tertiary interactions with T-loop residues (Helm et al. 2000) but presents G13 and A22 residues, characteristic of class II tRNA species[2] (Giegé et al. 1993). Both nucleotides are prone to pair via a *trans*-Hoogsteen/sugar edge interaction (Leontis et al. 2002) as seen in the crystal structure of *Thermus thermophilus* tRNA^{Tyr} (Yaremchuk et al. 2002). The T-loop consists of five nt instead of seven nt in classical tRNAs, and lacks both conserved C56 and A58 residues involved in long-range interactions (with G18 and U54, respectively).

[1]tRNA genes are distributed either on the heavy (G-rich) or light mt-DNA strand (C-rich). Transcription of the heavy DNA chain leads to 14 "light" mt-tRNAs and transcription of the light DNA chain leads to eight "heavy" mt-tRNAs (Anderson et al. 1981).

[2]Class II tRNAs (Leu, Ser, Sec, and bacterial Tyr) possess a large variable region (over 10 nt) in opposition to class I tRNAs with a small variable region (up to five nt).

Consequently, the 3D folding of this tRNA cannot involve classical D/T-loop interactions, and will likely be achieved via an alternative network, not yet identified, that may still include other classical tertiary interactions (see Fig. 1A; for review, see Helm et al. 2000). The pathogenic mutations G15A, A22G, and U54C in the human mt-tRNA^{Tyr} gene are located at positions usually involved in the classical tertiary interaction network. Notice further that the three residues are remote from the synthetase and excluded from a direct interaction in the interaction model proposed in Figure 1B. This model is based on the recently solved crystal structure of mt-TyrRS (Bonnefond et al. 2007b) combined with knowledge on tRNA^{Tyr}/TyrRS complexes showing a cross-subunit binding of the tRNA (Bedouelle 2005). Also, the location of all three residues in the tRNA differs from that of the tyrosine identity nucleotides. These latter, determining tyrosylation specificity and interacting with the synthetase, are found at the two distal ends of the tRNA (Bonnefond et al. 2005b). Given these facts, it can be hypothesized that the pathogenic mutations may induce a structural perturbation in mt-tRNA^{Tyr}, and therefore indirectly affect the tyrosylation ability of the mutants.

In this work, wild-type and mutated molecules were produced by in vitro transcription. Since transcripts do not contain the post-transcriptional modifications known to stabilize tRNA folding (e.g., Agris 1996) or induce the correct cloverleaf folding as shown for human mt-tRNA^{Lys} (Helm et al. 1998), one can wonder about the conformation of these molecules. Therefore, as a prerequisite to our study, we investigated whether the folding of the wild-type transcript was of the anticipated cloverleaf-type.

Probing of wild-type human mt-tRNA^{Tyr} structure

A wild-type mt-tRNA^{Tyr} transcript was probed with chemical (Pb^{2+}) and enzymatic probes (nucleases S1, T1, T2) known to preferentially cleave single-stranded regions, as well as with nuclease V1 specific of double-stranded and structured RNA regions (Giegé et al. 2001) (Fig. 2). The S1, T1, T2, and lead cleavage patterns show strong cuts in the anticodon-, T-, and D-loops, whereas the acceptor-, D-, T-, and anticodon arms are cleaved by nuclease V1 and are mainly insensitive to lead (Fig. 2A), thereby supporting the existence of the cloverleaf-fold depicted in Figure 1A. However, some residues within the tRNA arms (particularly the anticodon arm) are cut by the single strand-specific nucleases, and conversely, few residues located in D- and anticodon loops are recognized by nuclease V1, the probe specific for highly structured regions. Further, residues belonging to the anticodon arm are sensitive to Pb^{2+} cleavage, suggesting an opening of this region. These apparently contradictory data reflect the existence of alternate tRNA conformations in equilibrium with the canonical cloverleaf as previously shown in probing experiments conducted on other mt-tRNAs (e.g., human mt-tRNA^{Lys}) (Helm et al. 1998) and mt-tRNA$^{Leu(UUR)}$ (Sohm et al. 2003). However, the high tyrosylation level (over 80%, not shown) observed for the wild-type molecule reflects a large proportion of correctly folded transcripts

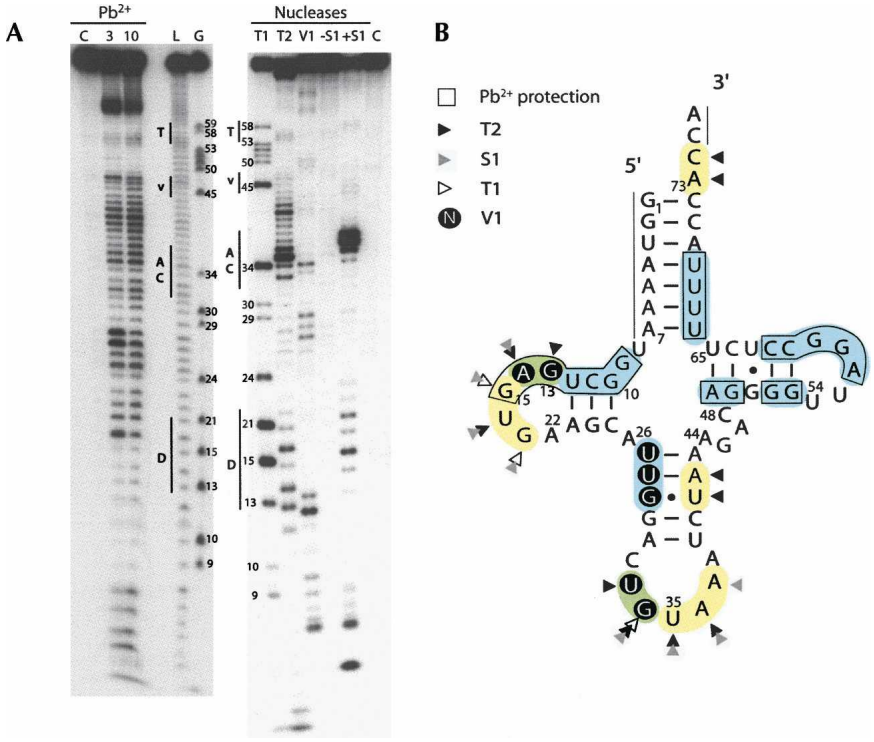

FIGURE 2. Probing of wild-type human mt-tRNA^{Tyr} transcript. (*A*) Autoradiogram of a 12% denaturing gel of probing experiments on 5′-labeled mt-tRNA^{Tyr}. Experiments were conducted at 25°C using Pb^{2+}, RNases T1, T2, and V1 and nuclease S1 as described in Théobald-Dietrich et al. (2004). Final concentrations of Pb^{2+} (in mM) are indicated. Control incubation (lane *C*) without probes was run in parallel. Lane −S1 is a control that checks the effect of $ZnCl_2$ present in nuclease S1 buffer. Lane *L* represents an alkaline ladder, and lane *G* represents a denaturing RNase T1 ladder (each G residue is numbered). D-loop (D), anticodon-loop (AC), variable region (v) and T-loop (T) are indicated by black vertical bars. (*B*) Summary of the probing experiments displayed on mt-tRNA^{Tyr} cloverleaf (only the strongest nuclease cuts and lead protections are taken into account for interpretation). Nucleotides cut by nucleases S1, T1, and T2 are indicated by triangles. White letters on black backgrounds emphasize cleavages by RNase V1. Regions resistant to Pb^{2+} cuts are boxed. Yellow areas correspond to nucleotides cut by nucleases specific for single-stranded regions. Blue areas correspond to nucleotides cut by V1 nuclease or insensitive to lead cleavage. Regions cut by both types of enzymatic probes are in green. Bars at the 3′- and 5′-ends indicate noninterpretable regions.

upon interaction with the synthetase. Notice the presence in control lanes of some faint hydrolytic cleavages (Fig. 2A) that become visible at PyA (Py for pyrimidine) positions when the autoradiogram is overexposed (data not shown).

Altogether, our data indicate that the wild-type human mt-tRNA^{Tyr} transcript is intrinsically structured, and folds preferentially in a cloverleaf despite the absence of post-transcriptional modifications (Fig. 2B). This interpretation is in line with the ranking of this molecule among the "heavy" mt-tRNAs with an excess of G-residues (on average 27%) as opposed to the "light" species (on average 14%) (Florentz et al. 2003), which consequently fold into less stable structures as, for example, human tRNA^{Lys} (Sissler et al. 2004).

Tyrosylation activity of wild-type and mutated human mt-tRNA^{Tyr} transcripts

Steady-state parameters for tyrosylation of these tRNA molecules by native human mt-TyrRS are summarized in Table 1. Whereas variant U54C behaves similarly to wild-type mt-tRNA^{Tyr}, substitutions of G15 by A, and especially of A22 by G, significantly affect the tyrosylation capacity of both molecules with losses in catalytic efficiency (k_{cat}/K_M) of 40- and 600-fold, respectively. Kinetic parameters revealed a predominant effect on k_{cat} (K_M only being affected up to sixfold) in accordance with that observed on other aminoacylation systems (e.g., Kelley et al. 2000; Sissler et al. 2004). Since direct interaction between residues 15, 22, and 54 and the cognate dimeric mt-TyrRS is unlikely (Fig. 1B), it implies that the reduced aminoacylation efficiency of the mutants occurs via structural perturbations that are a priori strongest for A22G, moderate for G15A, and negligible for U54C. To evaluate the structural changes responsible for the perturbed tyrosylation kinetics, we investigated the solution structure of each mutated tRNA molecule.

Architectural perturbations in the mutant human mt-tRNA^{Tyr} structures

The three mutated mt-tRNA^{Tyr} variants were probed under identical conditions in experiments run in parallel with the wild-type molecule. Comparisons reveal alterations in all cleavage patterns as depicted in Figure 3.

For the U54C mutant, changes in nuclease probing are faint and concern essentially residues 14–23 (D-loop), 57, 58 (T-loop), and G24 (D-stem) that all become less accessible to S1 and T1 nucleases, compared to wild-type transcript. The reduced accessibility of residues 53 and 54 is confirmed by the absence of Pb^{2+} cleavages at these positions. Further, residue U63 (T-arm) is seen more accessible to V1 in the mutated molecule. Despite these subtle changes, both U54C and wild-type patterns are globally similar (cf. Figs. 2A and 3A).

Second, mutant G15A and A22G exhibit similar nuclease cleavage profiles that however differ from that of the wild-type molecule. More precisely, both mutants show enhanced T2-cuts in the D-loop region (from residue 13–22) as well as new S1-cuts in the anticodon stem-region (from residue 13–44) not seen in the wild-type molecule. Further, in mutant G15A, residues 48–50 are accessible to V1 as well as nucleotide 15 that is more reactive to T2 nuclease. Regarding mutant A22G, residues G13 and G24 show enhanced cuts by T1. Finally, both mutants exhibit similar Pb^{2+} cleavage patterns that differ from the wild-type mt-tRNA^{Tyr} at positions 9–12 and 16 for G15A transcript and at positions 9 and 10 for A22G transcript.

Inspection of control lanes reveals significant differences in the distribution of hydrolytic cleavages (Figs. 2A, 3A). Whereas the wild-type and mutant U54C show almost no hydrolytic cuts, mutant G15A and A22G present a larger number. These cuts are of variable intensities and correspond mainly to PyA sequences in connecting regions as, for example, C25A26 and C48A49 (Fig. 3B). They reflect the accessibility of tRNA backbone to water molecules and especially the facilitated formation of cyclic phosphates due to a greater flexibility of the molecule (Dock-Bregeon and Moras 1987; Giegé et al. 2001).

Altogether, nucleases, lead, and hydrolytic cuts point toward an overall similar structural fold for both wild-type and U54C transcripts that differ from that of the G15A and A22G molecules. These latter are similar and present altered conformations together with an enhanced structural plasticity.

Toward understanding the structural role of residues G15, A22, and U54

Tyrosine identity determinants in human mt-tRNA^{Tyr} (anticodon G34 U35 A36 and discriminator A73) are located

TABLE 1. Tyrosylation by human mt-TyrRS of wild-type and pathology-related mt-tRNA^{Tyr} variants

mt-tRNA^{Tyr} transcripts	Gene mutation	K_M (μM)	k_{cat} ($10^{-3}\cdot sec^{-1}$)	k_{cat}/K_M ($10^{-3}\cdot s^{-1}\cdot \mu M^{-1}$)	L[a] (x-fold)
Wild type		4.8	46	9.6	1
G15A	C5877T	0.8	0.2	0.25	40
A22G	T5874C	1.6	0.03	0.016	600
U54C	A5843G	2.2	12	5.4	1.8

[a]L values correspond to losses of catalytic efficiency relative to wild-type human mt-tRNA^{Tyr}.

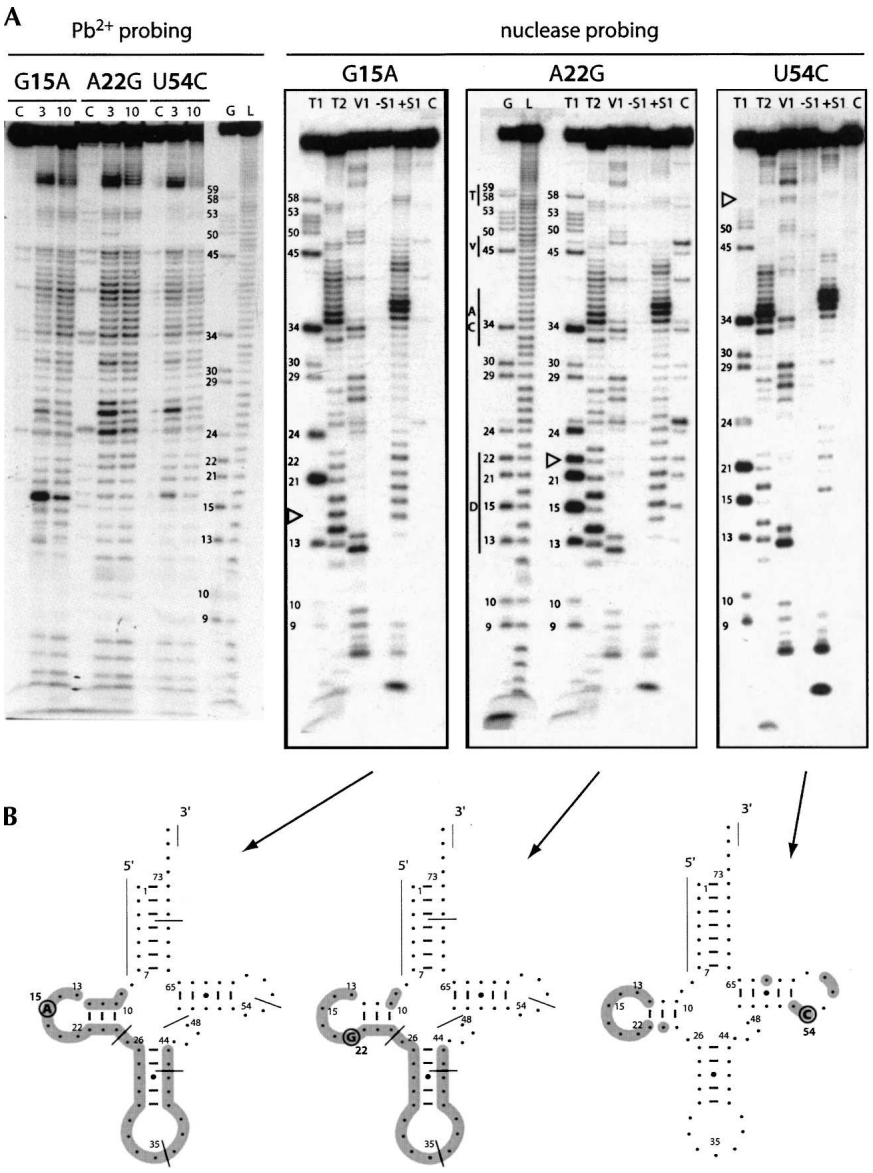

FIGURE 3. Structural analysis of mutants 15, 22, and 54. (*A*) Autoradiograms of 12% denaturing gels of probing experiments performed on mt-tRNA^{Tyr} G15A, A22G, and U54C variants. The *left* and *right* panels correspond to Pb^{2+} and nuclease probing, respectively. For annotations, see the legend of Figure 2A. The white triangles indicate the location of the pathogenic mutation in each molecule. (*B*) Interpretation of the cleavages on schematic cloverleaf folds. Nucleotides are represented by small dots (for the complete mt-tRNA^{Tyr} sequence, see Fig. 2B) except the mutated residue shown explicitly for each variant. Nucleotides showing strong increased or decreased cuts (compared to the wild-type mt-tRNA^{Tyr} molecule) are emphasized in gray. Strokes indicate positions of hydrolytic cuts. Bars at both 3′- and 5′-ends correspond to noninterpretable regions.

at the distal ends of the L-shaped tRNA (Bonnefond et al. 2005b). According to identity rules, specific aminoacylation results from a productive interaction between the identity nucleotides and the amino acids of the cognate synthetase (for review, see Giegé et al. 1998; Giegé and Frugier 2003). Given the proposed model, residues 15, 22, and 54 are not thought to directly contact the synthetase (Fig. 1B). Thus, mutations of these residues should not affect tyrosylation properties of the corresponding transcripts unless their tertiary structure is perturbed. This occurs with the U54C mutant that presents a probing pattern essentially similar to that of wild type. In the case of the G15A and A22G mutants, the losses in tyrosylation efficiency reflect a structural alteration. In what follows, we consider each mutation individually.

Residue U54 is conserved in the majority of cytosolic tRNAs where it interacts with A58 to give the proper conformation to the T-loop (for review, see Giegé and Frugier 2003). In human mt-tRNA^{Tyr}, residue U54 cannot fulfill this structural role due to the reduced size of the T-loop. Further, the nonconservation of this residue in mt-tRNA^{Tyr} species does not support a structural role of U54. Indeed, kinetic parameters for tyrosylation are not affected by the pathogenic mutation, confirming that the replacement of U by C does not perturb the overall structure of human mt-tRNA^{Tyr}. This agrees with a globally unchanged sensitivity of this tRNA to the structural probes. Therefore, the efficient tyrosylation activity of this mutant implies that the pathogenic mutation affects essential interaction(s) with other partner(s) of mt-tRNA^{Tyr}.

Residue G15, conserved in almost all mammalian mt-tRNA^{Tyr} sequences, is known to interact with C48 in the variable region of canonical tRNAs (Giegé and Frugier 2003). This tertiary interaction can be maintained in mt-tRNA^{Tyr} (Fig. 1A) since C48 is present. In the pathogenic mutant G15A, this pair is likely disrupted, as shown by the enhanced reactivity of both residues A15 and C48 in the mutant compared to the wild-type transcript. This disruption probably triggers a structural destabilization in both D-arms and anticodon arms as shown by the increased number of cuts in these regions that behave as single strands. This perturbation explains the decreased tyrosylation ability (40-fold) of the mutated transcript.

As found for class II tRNAs with large variable regions, pairing between A22 and G13 probably also occurs in human mt-tRNA^{Tyr}. Substituting A22G leads either to a larger and nonisosteric G13–G22 pair with only one H-bond

(Leontis et al. 2002) or to a total disruption. This latter hypothesis is favored, given the enhanced cuts observed for residues G13, G22, and G24. Similar to mutant G15A, the mutation triggers a structural change in the tRNA that propagates in a zipper-like fashion from the D-stem toward the anticodon stem, both seen more accessible to probes. Thus, the strong loss in tyrosylation for mutant A22G is due to a structural perturbation of the molecule and clearly indicates a key role of residue A22 in the 3D architecture of the mitochondrial tRNA, as is the case for mutation G15A.

Altogether, our data show that residue U54 does not contribute to the long-range tertiary network of mt-tRNA^{Tyr} as opposed to nucleotides G15 and A22. Both residues, located in the D-loop, probably stabilize the tRNA by making tertiary interactions with residues located in the variable region (C48) and in the D-loop (G13), respectively.

Final considerations

Only few studies relate to pathogenic mutations of mt-tRNA genes taking place in single-stranded regions and particularly in D- and T-loops. For example, mutation A10044G in mt-tRNA^{Gly} gene changing A58 into G in the T-loop weakens the interaction between D- and T-loops and therefore interferes with the CCA adding enzyme (Tomari et al. 2003). Further, mutation A4317G in mt-tRNA^{Ile} gene induces an alternative T-stem structure incompatible with aminoacylation (Kelley et al. 2001), a possibility favored by the structural fragility of the mt-tRNA (Kelley et al. 2000). In the case of mt-tRNA^{Tyr}, a direct implication of G15 and A22 in the tyrosylation process is ruled out based on crystallographic knowledge of the mt-TyrRS (Bonnefond et al. 2007b) and of *T. thermophilus* (Yaremchuk et al. 2002), *Methanococcus jannaschii* (Kobayashi et al. 2003), and cytosolic *Saccharomyces cerevisiae* (Tsunoda et al. 2007) tRNA^{Tyr}/TyrRS complexes. We show here that the aminoacylation deficiencies are due to structural perturbations and correspond to the initial impact of the mutations. Our study strengthens the fact that local perturbations either in stem or loop regions as well as chemical fragility of a mutated tRNA affect recognition by tRNA-specific enzymes. Despite the absence of crystallographic data, the combined result of structural probing and tyrosylation assays supports the existence of G13A22 and G15C48 tertiary interactions. The strong conservation of residues G13, G15, A22 (> 90%), and C48 (87%) in 150 mammalian mt-tRNA^{Tyr} species further supports this interpretation.

On the other hand, the pathogenic mutation U54C (A5843G in the gene) affects neither aminoacylation nor tRNA structure. Similarly, it has been reported that mutation A55G in mt-tRNA^{Lys} (A8344G in the gene) does not prevent in vitro aminoacylation by mt-LysRS (Sissler et al. 2004). Here, the deleterious effect of mutation U54C has to be sought among the multiple steps of the tRNA life cycle. Such knowledge is crucial to understand the pathogenic effect triggered by the mutation.

MATERIAL AND METHODS

Materials

All mt-tRNA^{Tyr} transcripts were produced in vitro using the "transzyme" method and purified as described in Fechter et al. (1998). Briefly, the synthetic genes composed of overlapping oligonucleotides contain a T7 RNA polymerase promoter followed by a hammerhead ribozyme and tRNA sequences. A BstNI site, coincidental with the 3′-end of the tRNA sequence, allows synthesis of tRNAs ending with the expected CCA-3′-sequence. After transcription, the hammerhead ribozyme self-cleaves and liberates the tRNA. Before use in functional and structural assays, tRNA transcripts were renatured by heating at 60°C for 90 sec in water followed by a slow cooling to room temperature.

The C-terminal His-tagged human mt-TyrRS was cloned, expressed, and purified as described elsewhere (Bonnefond et al. 2005a).

Aminoacylation assays

Tyrosylation assays were performed at 37°C in 50 mM HEPES-NaOH (pH 7.6) buffer containing 25 mM KCl, 12 mM $MgCl_2$, 2.5 mM ATP, 0.2 mg/mL bovine serum albumin, 1 mM spermine, and 10 μM L-[^{3}H]-tyrosine at 49 Ci/mmol (Sohm et al. 2003). Apparent kinetic parameters were determined from Lineweaver-Burk plots in the presence of mt-TyrRS (diluted in 100 mM HEPES-NaOH pH 7.4, 1 mM DTT, 5 mg/mL bovine serum albumin, and 10% glycerol) and transcript concentrations ranging from 0.2 to 2 μM. Depending on the degree of impairment of tRNA activity, mt-TyrRS concentrations varying from 75 nM to 1.5 μM were used. Experimental errors on k_{cat} and K_M varied at most by 20%. Numerical values are averages of at least two independent experiments.

Structural mapping procedures

Structural mapping of transcripts was done using chemical and enzymatic probes that preferentially cut single-stranded (Pb^{2+} and T1, S1, T2 nucleases) and double-stranded or highly structured domains (RNase V1). Labeling the 5′-end of mt-tRNA^{Tyr} transcripts was performed as described (Silberklang et al. 1977). Digestions of tRNAs with nucleases was for 10 min at 25°C in buffer T (25 mM KCl, 10 mM $MgCl_2$, and 50 mM HEPES-NaOH pH 7.5). For digestion with S1 nuclease, 1 mM $ZnCl_2$ was added. Reaction mixtures (10 μL) contained 100,000 Cerenkov cpm of transcript supplemented with 20 pmol of unlabeled tRNA and either 9×10^{-4} U RNase V1, 4.7 U nuclease S1, 0.18 U RNase T1, or 3.5×10^{-2} U RNase T2. Reactions were stopped on ice and by addition of 20 μL 0.6 M NaOAc, 4 mM EDTA, and 0.1 mg/mL total tRNA, followed by phenol extraction and ethanol precipitation of the tRNA. A freshly prepared $Pb(Oac)_2$ solution in H_2O was used at 3 and 10 mM final concentrations. Samples (10 μL) were incubated for 6 min at 25°C. Reactions were stopped by cooling on ice, adding EDTA to a final concentration of 33 mM and ethanol precipitated. Controls without probes were run in parallel on each gel.

For assignment of cleavage positions, alkaline degradations were performed by incubation of labeled transcripts for 4 min at 80°C in 50 mM $NaHCO_3$ pH 9.0. Guanine ladders were generated by RNase T1 digestion under denaturing conditions (Peattie and Gilbert 1980). All experiments were performed and run in parallel with the same nuclease and Pb^{2+} dilutions.

ACKNOWLEDGMENTS

We thank Marie Sissler for stimulating discussions. This work was supported by Centre National de la Recherche Scientifique (CNRS), Université Louis Pasteur de Strasbourg, and the French Ministry of Research (ACI ''BCMS'' 042358). L.B. was supported by a doctoral grant from the French Ministry for Research.

Received November 27, 2007; accepted December 19, 2007.

REFERENCES

Agris, P.F. 1996. The importance of being modified: Roles of modified nucleosides and Mg^{2+} in RNA structure and function. *Prog. Nucleic Acid Res. Mol. Biol.* **53:** 79–129.

Anderson, S., Bankier, A.T., Barrell, B.G., de Bruijn, M.H., Coulson, A.R., Drouin, J., Eperon, I.C., Nierlich, D.P., Roe, B.A., Sanger, F., et al. 1981. Sequence and organization of the human mitochondrial genome. *Nature* **290:** 457–465.

Bedouelle, H. 2005. Tyrosyl-tRNA synthetases. In *Aminoacyl-tRNA synthetases* (eds. M. Ibba et al.), pp. 111–124. Landes Biosciences, Georgetown, TX.

Bonnefond, L., Fender, A., Rudinger-Thirion, J., Giegé, R., Florentz, C., and Sissler, M. 2005a. Towards the full set of human mitochondrial aminoacyl-tRNA synthetases: Characterization of AspRS and TyrRS. *Biochemistry* **44:** 4805–4816.

Bonnefond, L., Giegé, R., and Rudinger-Thirion, J. 2005b. Evolution of the $tRNA^{Tyr}$/TyrRS aminoacylation systems. *Biochimie* **87:** 873–883.

Bonnefond, L., Frugier, M., Touzé, E., Lorber, B., Florentz, C., Giegé, R., Rudinger-Thirion, J., and Sauter, C. 2007a. Tyrosyl-tRNA synthetase: The first crystallization of a human mitochondrial aminoacyl-tRNA synthetase. *Acta Crystallogr.* **F63:** 338–341.

Bonnefond, L., Frugier, M., Touzé, E., Lorber, B., Florentz, C., Giegé, R., Sauter, C., and Rudinger-Thirion, J. 2007b. Crystal structure of human mitochondrial tyrosyl-tRNA synthetase reveals common and idosyncratic features. *Structure* **15:** 1505–1516.

Brandon, M.C., Lott, M.T., Nguyen, K.C., Spolin, S., Navathe, S.B., Baldi, P., and Wallace, D.C. 2005. MITOMAP: A human mitochondrial genome database—2004 update. *Nucleic Acids Res.* **33:** D611–D613. doi: 10.1093/nar/gki079.

Chinnery, P.F. and Turnbull, D.M. 2000. Mitochondrial DNA mutations in the pathogenesis of human disease. *Mol. Med. Today* **6:** 425–432.

Dock-Bregeon, A.C. and Moras, D. 1987. Conformational changes and dynamics of tRNAs: Evidence from hydrolysis patterns. *Cold Spring Harb. Symp. Quant. Biol.* **52:** 113–121.

Fechter, P., Rudinger, J., Giegé, R., and Théobald-Dietrich, A. 1998. Ribozyme processed tRNA transcripts with unfriendly internal promoter for T7 RNA polymerase: production and activity. *FEBS Lett.* **436:** 99–103.

Florentz, C. and Sissler, M. 2001. Disease-related versus polymorphic mutations in human mitochondrial tRNAs. Where is the difference? *EMBO Rep.* **2:** 481–486.

Florentz, C., Sohm, B., Tryoen-Tóth, P., Pütz, J., and Sissler, M. 2003. Human mitochondrial tRNAs in health and disease. *Cell. Mol. Life Sci.* **60:** 1356–1375.

Giegé, R. and Frugier, M. 2003. Transfer RNA structure and identity. In *Translation mechanisms* (eds. J. Lapointe and L. Brakier-Gringas), pp. 1–24. Landes Sciences, Georgetown, TX.

Giegé, R., Puglisi, J.D., and Florentz, C. 1993. tRNA structure and aminoacylation efficiency. *Prog. Nucleic Acid Res. Mol. Biol.* **45:** 129–206.

Giegé, R., Sissler, M., and Florentz, C. 1998. Universal rules and idiosyncratic features in tRNA identity. *Nucleic Acids Res.* **26:** 5017–5035. doi: 10.1093/nar/26.22.5017.

Giegé, R., Helm, M., and Florentz, C. 2001. Classical and novel chemical tools for RNA structure probing. In *RNA* (eds. D. Söll et al.), pp. 71–89. Elsevier Science B.V, Amsterdam.

Helm, M., Brulé, H., Degoul, F., Cepanec, C., Leroux, J.-P., Giegé, R., and Florentz, C. 1998. The presence of modified nucleotides is required for cloverleaf folding of a human mitochondrial tRNA. *Nucleic Acids Res.* **26:** 1636–1643. doi: 10.1093/nar/26.7.1636.

Helm, M., Brulé, H., Friede, D., Giegé, R., Pütz, J., and Florentz, C. 2000. Search for characteristic structural features of mammalian mitochondrial tRNAs. *RNA* **6:** 1356–1379.

Jacobs, H.T. and Holt, I.J. 2000. The np 3243 MELAS mutation: Damned if you aminoacylate, damned if you don't. *Hum. Mol. Genet.* **9:** 463–465.

Kelley, S.O., Steinberg, S.V., and Schimmel, P. 2000. Functional defects of pathogenic human mitochondrial tRNAs related to structural fragility. *Nat. Struct. Biol.* **7:** 862–865.

Kelley, S.O., Steinberg, S.V., and Schimmel, P. 2001. Fragile T-stem in disease-associated human mitochondrial tRNA sensitizes structure to local and distant mutations. *J. Biol. Chem.* **276:** 10607–10611.

Kobayashi, T., Nureki, O., Ishitani, R., Yaremchuk, A., Tukalo, M., Cusack, S., Sakamoto, K., and Yokoyama, S. 2003. Structural basis for orthogonal tRNA specificities of tyrosyl-tRNA synthetases for genetic code expansion. *Nat. Struct. Biol.* **10:** 425–432.

Leontis, N.B., Stombaugh, J., and Westhof, E. 2002. The non-Watson–Crick base pairs and their associated isostericity matrices. *Nucleic Acids Res.* **30:** 3497–3531. doi: 10.1093/nar/gkf481.

Levinger, L., Mörl, M., and Florentz, C. 2004. Mitochondrial tRNA 3′ end metabolism and human disease. *Nucleic Acids Res.* **32:** 5430–5441. doi: 10.1093/nar/gkh884.

McFarland, R., Elson, J.L., Taylor, R.W., Howell, N., and Turnbull, D.M. 2004. Assigning pathogenicity to mitochondrial tRNA mutations: When ''definitely maybe'' is not good enough. *Trends Genet.* **20:** 591–596.

Peattie, D.A. and Gilbert, W. 1980. Chemical probes for higher-order structure in RNA. *Proc. Natl. Acad. Sci.* **77:** 4679–4682.

Pulkes, T., Siddiqui, A., Morgan-Hughes, J.A., and Hanna, M.G. 2000. A novel mutation in the mitochondrial $tRNA^{Tyr}$ gene associated with exercise intolerance. *Neurology* **55:** 1210–1212.

Pütz, J., Dupuis, B., Sissler, M., and Florentz, C. 2007. Mamit-tRNA, a database of mammalian mitochondrial tRNA primary and secondary structures. *RNA* **13:** 1184–1190.

Raffelsberger, T., Rossmanith, W., Thaller-Antlanger, H., and Bittner, R.E. 2001. CPEO associated with a single nucleotide deletion in the mitochondrial $tRNA^{Tyr}$ gene. *Neurology* **57:** 2298–2301.

Sahashi, K., Yoneda, M., Ohno, K., Tanaka, M., Ibi, T., and Sahashi, K. 2001. Functional characterisation of mitochondrial $tRNA^{Tyr}$ mutation (5877 → GA) associated with familial chronic progressive external ophthalmoplegia. *J. Med. Genet.* **38:** 703–705.

Scaglia, F., Vogel, H., Hawkins, E.P., Vladutiu, G.D., Liu, L.L., and Wong, L. 2003. Novel homoplasmic mutation in the mitochondrial $tRNA^{Tyr}$ gene associated with atypical mitochondrial cytopathy presenting with focal segmental glomerulosclerosis. *Am. J. Med. Genet.* **123A:** 172–178.

Silberklang, M., Gillum, A.M., and RajBhandary, U.L. 1977. The use of nuclease P_1 in sequence analysis of end group labeled RNA. *Nucleic Acids Res.* **4:** 4091–4108. doi: 10.1093/nar/4.12.4091.

Sissler, M., Helm, M., Frugier, M., Giegé, R., and Florentz, C. 2004. Aminoacylation properties of pathology-related variants of human mitochondrial $tRNA^{Lys}$ variants. *RNA* **10:** 841–853.

Sohm, B., Frugier, M., Brulé, H., Olszak, K., Przykorska, A., and Florentz, C. 2003. Towards understanding human mitochondrial leucine aminoacylation identity. *J. Mol. Biol.* **328:** 995–1010.

Sprinzl, M. and Vassilenko, K.S. 2005. Compilation of tRNA sequences and sequences of tRNA genes. *Nucleic Acids Res.* **33:** D139–D140. doi: 10.1093/nar/gki012.

Taylor, R.W. and Turnbull, D.M. 2005. Mitochondrial DNA mutations in human disease. *Nat. Rev. Genet.* **6:** 389–402.

Théobald-Dietrich, A., Frugier, M., Giegé, R., and Rudinger-Thirion, J. 2004. Atypical archaeal tRNA pyrrolysine transcript behaves towards EF-Tu as a typical elongator tRNA. *Nucleic Acids Res.* **32:** 1091–1096. doi: 10.1093/nar/gkh266.

Tomari, Y., Hino, N., Nagaike, T., Suzuki, T., and Ueda, T. 2003. Decreased CCA-addition in human mitochondrial tRNAs bearing a pathogenic A4317G or A10044G mutation. *J. Biol. Chem.* **278:** 16828–16833.

Tsunoda, M., Kusakabe, Y., Tanaka, N., Ohno, S., Nakamura, M., Senda, T., Moriguchi, T., Asai, N., Sekine, M., Yokogawa, T., et al. 2007. Structural basis for recognition of cognate tRNA by tyrosyl-tRNA synthetase from three kingdoms. *Nucleic Acids Res.* **35:** 4289–4300. doi: 10.1093/nar/gkm417.

Wallace, D.C. 1999. Mitochondrial diseases in man and mouse. *Science* **283:** 1482–1488.

Wittenhagen, L.M. and Kelley, S.O. 2003. Impact of disease-related mitochondrial mutations on tRNA structure and function. *Trends Biochem. Sci.* **28:** 605–611.

Yaremchuk, A., Kriklivyi, I., Tukalo, M., and Cusack, S. 2002. Class I tyrosyl-tRNA synthetase has a class II mode of cognate tRNA recognition. *EMBO J.* **21:** 3829–3840.